IEEE Photonics Journal
An IEEE Photonics Society Publication

Open Access

Experimental Demonstration of OFDM/OQAM Transmission for Visible Light Communications

Volume 8, Number 5, October 2016

Bangjiang Lin
Xuan Tang
Zabih Ghassemlooy, *Senior Member, IEEE*
Xi Fang
Chun Lin
Yiwei Li
Shihao Zhang

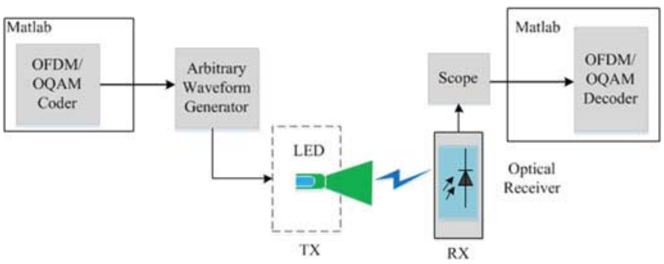

DOI: 10.1109/JPHOT.2016.2605464
1943-0655

IEEE photonics SOCIETY
IEEE

Experimental Demonstration of OFDM/OQAM Transmission for Visible Light Communications

Bangjiang Lin,[1] Xuan Tang,[1]
Zabih Ghassemlooy,[2] *Senior Member, IEEE*, Xi Fang,[3] Chun Lin,[1]
Yiwei Li,[1] and Shihao Zhang[1]

[1]Quanzhou Institute of Equipment Manufacturing, Haixi Institutes, Chinese Academy of Sciences, Quanzhou, 362200, China
[2]Optical Communications Research Group, NCRLab, Faculty of Engineering and Environment, Northumbria University, Newcastle NE1 8ST, U.K.
[3]State Key Laboratory of Advanced Optical Communication Systems and Networks, Peking University, Beijing 100871, China

DOI:10.1109/JPHOT.2016.2605464

Manuscript received June 30, 2016; revised August 29, 2016; accepted August 30, 2016. Date of publication September 2, 2016; date of current version September 22, 2016. This work was supported in part by the State Key Laboratory of Advanced Optical Communication Systems and Networks, China, and in part by the National Natural Science Foundation of China under Grant 61601439 and Grant 61501427. Corresponding author: B. Lin (e-mail: linbangjiang@163.com)

Abstract: We propose a modified orthogonal frequency division multiplexing/offset quadrature amplitude modulation (OFDM/OQAM) scheme for visible light communications (VLC). The OFDM/OQAM VLC system can efficiently boost the data rate, and combat multipath induced the inter symbol interference (ISI) and inter carrier interference (ICI). To combat the effect of intrinsic imaginary interference, intrasymbol frequency-domain averaging and minimum mean squared error (MMSE), combined with interference approximation method, are proposed. The experiment results show that the proposed system offers similar bit error rate performance to that of OFDM, while the bit rate is increased by 9% for the elimination of cyclic-prefix and guard band.

Index Terms: Offset quadrature amplitude modulation (OQAM), orthogonal frequency division multiplexing access (OFDM), visible light communications (VLC)

1. Introduction

Solid-state based light-emitting diodes (LEDs) have been considered as the most promising lighting source for next-generation illumination at a global level. This is because of the high luminance efficiency, longer life, low cost, and low power consumption. Additionally, LEDs have a unique feature of fast switching that has been effectively exploited for data communications. LED based visible light communications (VLC) has emerged as one of the key areas of this new photonics age, which take advantage of the new white LED-based lighting systems to provide data communications, sensing and localization at the same time. VLC offers advantages including unregulated huge spectrum as an alternative to the limited radio frequency spectrum, spectral re-use, immunity to the electromagnetic interference, inherent security against eavesdropping, etc. [1]–[2]. These features make VLC a strong candidate in future smart cities. As a bottleneck in conventional indoor VLC systems, the bandwidth of LEDs have recently increased from a few megahertz to several hundred megahertz by combination of a blue filter at the receiver (Rx) and equalizers both at the transmitter (Tx) and Rx, thus making very high-speed communications possible [3]–[5].

The orthogonal frequency division multiplexing (OFDM) scheme widely and successfully used in radio frequency (RF) systems [6]–[7] has also been adopted in VLC systems to further increase the bandwidth efficiency and overcome multipath induced inter symbol interference (ISI) and inter carrier interference (ICI) [8]–[10]. OFDM converts a frequency-selective channel into a set of parallel frequency-flat channels. Provided the cyclic-prefix (CP) is longer than the maximum delay introduced by the channel, the data at each sub-carrier can be equalized independently using a simple one-tap equalizer. However, insertion of CP will lead to reduced spectral efficiency. For the virtue of higher spectrum efficiency brought by the elimination of CP and lower out of band radiation using a specially designed filter bank, OFDM/offset quadrature amplitude modulation (OFDM/OQAM) has been considered as an attractive alternative to conventional OFDM [11]–[12]. To date, OFDM/OQAM systems has already been introduced in the digital ratio technical standards [13], wireless regional area network (WRAN IEEE 802.22) [14], and coherent optical communications [15]–[17]. In this paper, to the best of our knowledge, for the first time, we propose a modified OFDM/OQAM for intensity modulation and direct detection (IM/DD) VLC systems. Interference approximation method (IAM) is used to combat the effect of intrinsic imaginary interference (IMI), due to its low computational complexity and promising robustness against ISI by boosting the power of the “pseudo pilot”. To further increase the accuracy of channel estimation (CE), intra-symbol frequency-domain averaging (ISFA) and minimum mean squared error (MMSE) are combined with IAM. Both ISFA and MMSE perform channel estimation based on the channel frequency response obtained from IAM. Therefore, there is no need for an additional preamble in order to improve the spectral efficiency. With ISFA estimator, averaging is carried out over the estimated matrix for multiple adjacent frequency subcarriers (SCs), whereas with MMSE estimator, additional information such as the signal-to-noise ratio (SNR) and statistical characteristics of the channel are required. We show by experiment that the proposed VLC system offers increased bit rate by 9% and mitigate both ISI and ICI.

The rest of the paper is organized as follows. In Section 2, we introduce the modified OFDM/OQAM scheme for VLC systems. The IAM, ISFA and MMSE channel estimation methods are described in Section 3. Section 4 presents the experiment setup and results for OFDM/OQAM VLC, followed by the concluding remarks in Section 5.

2. Modified OFDM/OQAM Scheme

Fig. 1 shows the schematic block diagram of the proposed OFDM/OQAM system. The transmitted signal can be given as [13]–[17]

$$s(t) = \sum_{n=0}^{2Ns-1} \sum_{m=0}^{M-1} d_{m,n} \underbrace{g(t - n\tau_0) e^{j2\pi m v_0 t} e^{j\frac{\pi}{2}(m+n)}}_{g_{m,n}(t)} \tag{1}$$

where N_s denotes the number of baseband symbols, M is the number of total SCs $d_{m,n}$ is the real-valued transmitted symbol of the m-th SC in the n-th OFDM/OQAM block selected from the real or the imaginary part of the data symbols. n is equal to $2k$ and $2k+1$ for the real and imaginary part, respectively. v_0 and τ_0 represent the SC spacing in each OFDM/OQAM block and the OQAM symbol duration, respectively. $g(t)$ is the prototype filter, which is well localized in both time and frequency domains for OFDM/OQAM signals [18]. The basis function $g_{m,n}(t)$ is the shifted version of $g(t)$ in both time and frequency domains, and the orthogonal condition only holds in the real field in [19] and is given by

$$\begin{aligned} \mathrm{Re}\left\{\langle g_{m,n}, g_{m+p,\, n+q}\rangle\right\} &= \mathrm{Re}\left\{\int g_{m,n}(t)\, g_{m+p,\, n+q}{}^{*}(t)\, dt\right\} \\ &= \begin{cases} 1, & (p, q) = (0, 0) \\ 0, & (p, q) \neq (0, 0) \end{cases} \end{aligned} \tag{2}$$

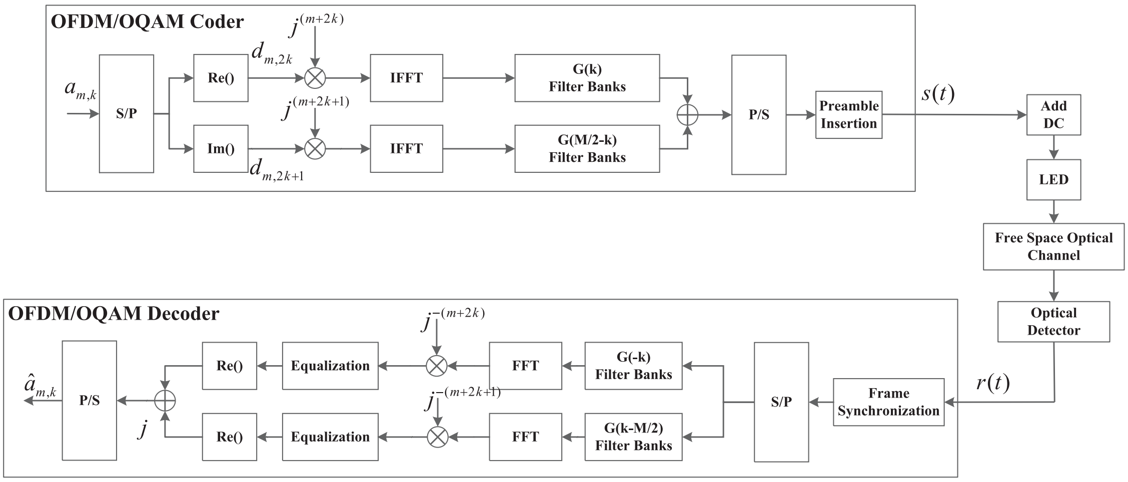

Fig. 1. Schematic diagram of OFDM/OQAM VLC systems. (S/P: serial-to-parallel conversion, P/S: parallel-to-serial conversion.)

where Re(X) represents the real part of vector X. We define the pure imaginary term $\langle g_{m,n}, g_{m+p,\,n+q}\rangle = j\langle g\rangle_{m,n}^{m+p,\,n+q}$ as the interference weight. In order to obtain a real value OFDM/OQAM signal, the input of data block should satisfy:

$$d_{m,n} = \begin{cases} 0, \text{ if } m = 0, M/2 \\ (-1)^n d_{M-m,n}, \text{ otherwise,} \end{cases} \tag{3}$$

Hence, $M/2+1$ of SCs cannot be used to carry transmitted data. The preamble is required at the start of each OFDM/OQAM frame for CE and synchronization. Following direct current (DC) biasing, the DC-OFDM/OQAM is used for IM of the LED. Following propagation through the free space channel, the received DC-OFDM/OQAM signal is given as

$$r(t) = h(t) \otimes s(t) + \eta(t) \tag{4}$$

where $h(t)$ denotes the wireless free space channel response, $\eta(t)$ is the additive white Gaussian noise (AWGN), and the symbol $\otimes$ represents the convolution operation. The received OFDM/OQAM signal is first passed through a frame synchronization module prior to demodulation. The demodulated OFDM/OQAM signal is given as

$$\begin{aligned} r_{m,n} &= \int g_{m,n}{}^*(t)\,\{h(t) \otimes s(t)\,dt\} + \int g_{m,n}{}^*(t)\eta(t)\,dt \\ &= H_{m,n}d_{m,n} + \sum_{(p,q)\neq(0,0)} H_{m+p,\,n+q}d_{m+p,\,n+q}\left\langle g_{m,\,n}, g_{m+p,\,n+q}\right\rangle + \eta_{m,n} \end{aligned} \tag{5}$$

where the noise term is given as

$$\eta_{m,n} = \int g_{m,n}{}^*(t)\eta(t)\,dt. \tag{6}$$

For a symbol at the position $(m+p,\,n+q)((p,q) \in \Omega_{(1,1)})$, the following assumption for the frequency response of channel is always satisfied:

$$H_{m+p,\,n+q} \approx H_{m,n}. \tag{7}$$

Here, $\Omega_{(1,1)}$ represents the first order neighbor of $(0,0)$ as $\Omega_{(1,1)} = \{(p,q)||p| \leq 1 \text{ and } |q| \leq 1\}$. Since the prototype filter has good time-frequency localization (TFL) properties, as described in

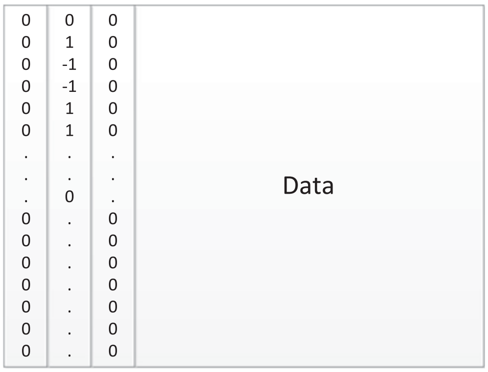

Fig. 2. Frame configuration for OFDM/OQAM VLC systems.

[19], we can obtain

$$\langle g_{m,n}, g_{m+p,\, n+q} \rangle \approx 0,\ (p, q) \notin \Omega_{(1,1)}. \tag{8}$$

We define $\Omega^*_{(1,1)} = \Omega_{(1,1)} - (0, 0)$. Thus, (5) can be further abbreviated as

$$r_{m,n} \approx H_{m,n} d_{m,\, n} + \underbrace{\sum_{(p,q)\in\Omega^*_{1,1}} H_{m,n} d_{m+p,\, n+q} \langle g_{m,n}, g_{m+p,\, n+q} \rangle}_{\text{IMI}} + \eta_{m,n}. \tag{9}$$

Equation (9) can be rewritten as

$$r_{m,n} = H_{m,n} \left(d_{m,n} + d^{(i)}{}_{m,n} \right) + \eta_{m,n}. \tag{10}$$

Here, the definition of the pure imaginary term $d^{(i)}{}_{m,n}$ is given as

$$d^{(i)}{}_{m,n} = \sum_{(p,q)\in\Omega^*_{1,1}} d_{m+p,\, n+q} \langle g_{m,n}, g_{m+p,\, n+q} \rangle. \tag{11}$$

If the channel state information could be accurately obtained resorting to the preambles that is being added at the start of each frame, the received data with channel equalization can be given as

$$\widehat{d}_{m,n} = \mathrm{Re}\left\{ H_{m,n}{}^{-1} r_{m,n} \right\}. \tag{12}$$

Then the real and imaginary parts are combined to obtain the received baseband symbols as shown in Fig. 1.

3. Proposed Channel Estimation Schemes

From (9), we can observe that to realize effective channel estimation for the OFDM/OQAM VLC system, the effect of IMI in (9) should be effectively suppressed by the utilization of specially designed preamble with no additional computational complexity. In order to suppress IMI, "pseudo pilots" in the form of $t_{m,n} + t^{(i)}{}_{m,n}$ are inserted in the preamble, and $t^{(i)}{}_{m,n}$ can be computed according to (11). A simple way to generate "pseudo pilots" would be to transmit three known consecutive OFDM/OQAM blocks ($t_{m,n-1}\ t_{m,n}\ t_{m,n+1}$) as the preamble, as shown in Fig. 2, where the first and the third preambles are placed with nulls, and the middle preamble satisfy

$$t_{m,n} = \begin{cases} 0, \text{ if } m = 0, M/2 \\ 1, \text{ if } m = 1, 4, 5 \\ -1, \text{ if } m = 2, 3 \\ t_{m-4,n}, \text{ if } m = 6 \cdots M/2 - 1 \\ (-1)^n t_{M-m,n}, \text{ otherwise.} \end{cases} \tag{13}$$

This ensures that the transmitted signal is real-value while decreasing the influence of the AWGN on the CE accuracy by increasing the power of the “pseudo pilots”. The received “pseudo pilots” can be given as

$$y_{m,n} = H_{m,n}\left(t_{m,n} + t^{(i)}{}_{m,n}\right) + \eta_{m,n} \tag{14}$$

where the imaginary interference for $t_{m,n}$ is given as

$$t^{(i)}{}_{m,n} = \sum_{(p,q)\in\Omega^*{}_{1,1}} t_{m+p,n+q}\left\langle g_{m,n}, g_{m+p,n+q}\right\rangle. \tag{15}$$

Thus channel estimation for the OFDM/OQAM VLC system can be performed as

$$\hat{H}_{IAM_{m,n}} = \frac{y_{m,n}}{t_{m,n} + t^{(i)}{}_{m,n}}. \tag{16}$$

Based on $\hat{\mathbf{H}}_{\mathrm{IAM}}$, ISFA and MMSE methods are used to increase the channel estimation accuracy. For the link with ISFA, the channel frequency response (CFR) is given by

$$\hat{H}_{ISFA_{m,n}} = \frac{\sum_{p=m-num}^{m+num} \hat{H}_{IAM_{p,n}}}{\max(M-1, m+num) - \min(0, m-num) + 1} \tag{17}$$

where *num* is the number of the left and right adjacent SCs that are employed for averaging in the frequency-domain, and $M-1$ and 0 are the maximum and minimum modulated subcarrier indexes, respectively. In Equation (17), the elements of the estimated channel matrix for p outside $[0, M-1]$ are not available and thus are set to zero in the averaging process. The frequency averaging reduces the fluctuation of the channel estimation caused by noise thus improves the CE accuracy. In addition, no additional pilot is required which improve the spectral efficiency. Equation (14) is very similar to a signal received in an OFDM system. Therefore, by analogy with the MMSE channel estimation obtained from the least square (LS) estimation in [20], it can be directly deduced from Equation (14) a simple expression of the MMSE estimation in OFDM/OQAM, as expressed below:

$$\hat{\mathbf{H}}_{MMSE_n} = \mathbf{R}_{hh}(\mathbf{R}_{hh} + \sigma_n^2(\mathbf{T_n}\mathbf{T_n}^H))^{-1})^{-1}\hat{\mathbf{H}}_{IAM_n}. \tag{18}$$

where $\mathbf{R}_{hh}$ is the auto-covariance matrix of $\hat{\mathbf{H}}_{\mathrm{MMSE}}$, σ_n^2 is the noise variance, and $\mathbf{T_n}$ is the $M \times M$ diagonal matrix containing the samples $t_{m,n} + t^{(i)}{}_{m,n}$ on its diagonal. As shown in Equation (18), the high complexity and the requirement of prior knowledge of $\mathbf{R}_{hh}$ and σ_n^2 limits the implementation of this MMSE method. To reduce the complexity, the low-rank approximation (LRA) method proposed in [21] is used to perform the MMSE estimation, in which an approximated auto-covariance matrix $\hat{\mathbf{R}}_{hh}$ instead of $\mathbf{R}_{hh}$ and a fixed approximated value $\hat{\sigma_n^2}$ are consider. Therefore, $\mathbf{R}_{hh}(\mathbf{R}_{hh} + \sigma_n^2(\mathbf{T_n}\mathbf{T_n}^H))^{-1})^{-1}$ can be computed offline only once and stored in the receiver. Therefore, the totally needed multiplications for CE are $M \times M + M$. In the IAM method, the totally necessary multiplications are M, while M multiplications and $M \times (2num + 1)$ additions are required for the ISFA method.

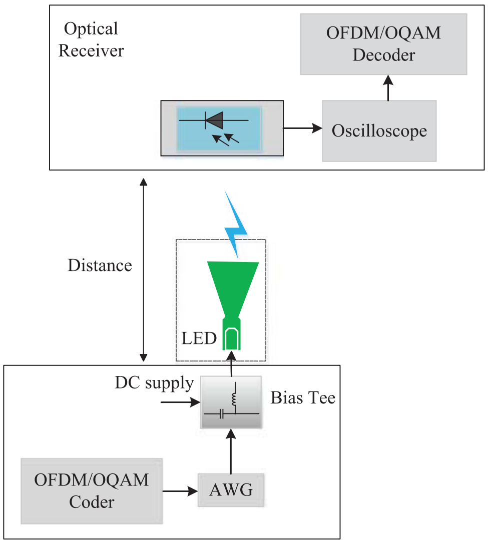

Fig. 3. Experiment setup for OFDM/OQAM-VLC.

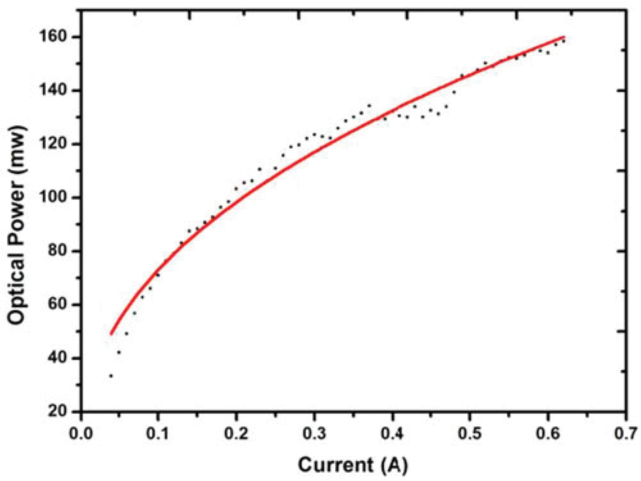

Fig. 4. Output optical power as a function of current.

4. Experiment Setup and Results

The experimental setup for OFDM/OQAM VLC is shown in Fig. 3. At the Tx, a 1 Mbaud baseband OFDM/OQAM signal with QPSK mapping is generated in the MATLAB domain, which is then uploaded onto an arbitrary waveform generator (AWG) operating at 1MS/s. The output of AWG (i.e., electrical OFDM/OQAM signal) is converted into an analog stream and then DC-level shifted prior to IM of a commercially available phosphorescent white LED (CRE EXML2). The total SCs employed are 256, of which 127 SCs are used for data transmission. The isotropic orthogonal transform algorithm (IOTA) given in [17] is adopted as the prototype filter to construct the filter banks. The pulse length of the prototype filter is $L = 4M = 1024$. Each frame contains $Ns = 30$ baseband data blocks, one block for synchronization and 1.5 training blocks for CE. The total bit rate $B_T = 30/32.5 \times 127/256 \times 2 \times 1\text{M} = 0.916$ Mb/s. The *P-I* characteristics of the LED is shown in Fig. 4, where the most linear part is with the current range of 0.15 – 0.6 A. The 3 dB modulation bandwidth of the LED is about 700 kHz, as shown in Fig. 5. The bandwidth can be extended

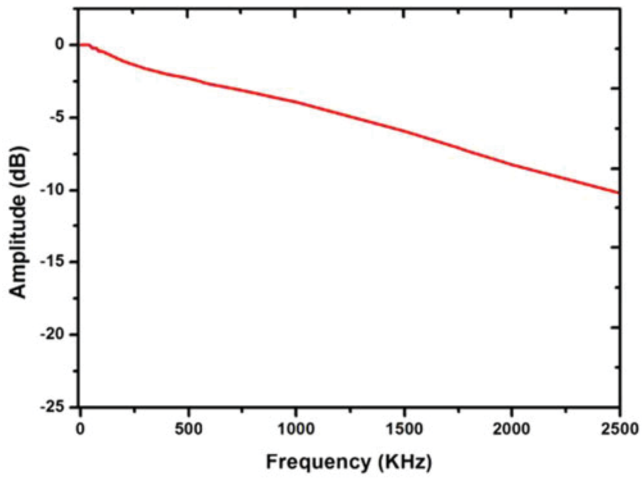

Fig. 5. Frequency response of the VLC system.

TABLE 1
System Parameters

Parameter	OFDM/OQAM	OFDM
No. of SCs (i.e., FFT size)	256	256
No. of SCs for data transmission	127	122
Prototype filter	IOTA	Rectangular
CP size	0	16
Symbol rate	1 Mbaud	1 Mbaud
Modulation	QPSK	QPSK
Bit rate	0.916 Mb/s	0.841 Mb/s
3 dB LED bandwidth	700 kHz	700 kHz
LED transmit power	100 mW	100 mW
DC bias	0.45 A	0.45 A
Photodetector responsivity	$<$0.44 A/W	$<$0.44 A/W
Rx bandwidth	150 MHz	150 MHz

using pre-equalization and post-equalization technologies [5]. In addition, multiple-input multiple-output (MIMO) and wavelength division multiplexing (WDM) can enhance the overall data rate by increasing the bandwidth efficiency [22], [23]. At the Rx, a commercial optical Rx (THORLABS PDA10A) composed of a Si photodetector and an amplifier is used to detect the optical signal, the output of which is passed through digital to analog converter (DAC) and captured using a real-time digital oscilloscope for offline signal processing in the MATLAB domain in order to recover the transmitted data. Note that the OFDM/OQAM decoder is exactly the opposite of the OFDM/OQAM encoder adopted at the Tx. All the key system parameters are shown in Table 1.

Also considered here is OFDM VLC transmission over a transmission span of 5–12 cm. The baseband 1 Mbaud QPSK-OFDM signal is also generated in MATLAB. In order to generate real-value OFDM signal Hermitian symmetry is applied to the signal prior to IFFT. Both the 0th and 128th

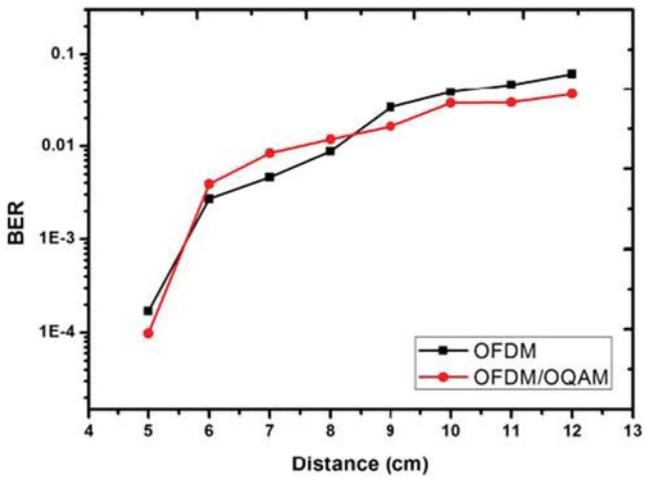

Fig. 6. BER performance as a function of distance for both OFDM and OFDM/OQAM.

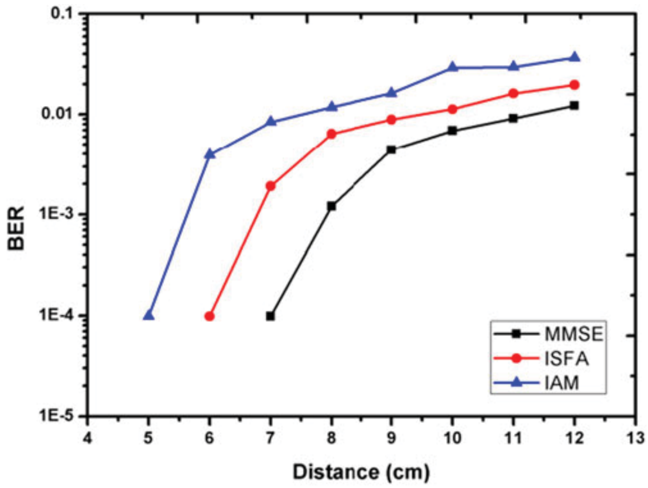

Fig. 7. BER performance for OFDM/OQAM-VLC with IAM, ISFA, and MMSE.

SCs carry no data, whereas123-127th SCs are used as guard band, 1-122th SCs are used for data transmission, and 129-255th SCs carry the complex conjugate of data on the 1-127th SCs. Due to the out of band radiation, the guard band is necessary in OFDM VLC systems. Otherwise, the transmission performance would be degraded. The training symbols with real-values are required at the start of each OFDM frame for the purpose of CE and synchronization. Each frame contains 30 OFDM blocks, one block each for synchronization and channel estimation. The total bit rate $B_T = 30/32 \times 122/256 \times 256/272 \times 2 \times 1$ M $= 0.841$ Mb/s. The least square (LS) channel estimation method is considered here. The optical transceiver and the channel adopted here are the same as that of OFDM/OQAM; see Fig. 3.

The bit error rate (BER) performance against the transmission span for both OFDM and OFDM/OQAM VLC schemes are shown in Fig. 6. Each BER point is determined from 10 frames, with a total of more than 5×10^4 bits. We can see that OFDM/OQAM has similar BER performance to that of OFDM. However, OFDM/OQAM offers increased bit rate by 9% due to the elimination of CP and guard band. Fig. 7 shows the BER performance for OFDM/OQAM-VLC with IAM, ISFA, and MMSE. Both ISFA and MMSE outperform the conventional IAM method, because of more accurate

CE. Note that in the ISFA, the estimation results from IAM are used along with the averaging of five adjacent subcarriers. Compared with IAM, the increased transmission spans at a BER of 10^{-4} are about 1cm and 2 cm for ISFA and MMSE, respectively.

5. Conclusion

In this paper, for the first time, we introduce the OFDM/OQAM scheme for the VLC system. As a good alternative for conventional OFDM, OFDM/OQAM can also increase the bandwidth efficiency and overcome multipath induced IS and ICI. Compared with single carrier based VLC systems, such as on-off keying, pulse width modulation and pulse position modulation, OFDM/OQAM VLC systems offer higher spectral efficiency and high tolerance against multipath distortion. Contrary to the OFDM VLC systems which use a CP to combat time dispersion, OFDM/OQAM VLC systems utilize well designed pulse shapes but no CP and guard band, hence, have the advantages of reduced out-of-band energy and a higher spectral efficiency. The experiment results showed that the OFDM/OQAM VLC system displayed similar performance to that of OFDM but with 9% increased bit rate due to the elimination of CP and guard band. To combat the effect of IMI, we introduced ISFA and MMSE which outperformed the conventional IAM.

References

[1] A. Jovicic, J. Li, and T. Richardson, "Visible light communication: Opportunities, challenges and the path to market," *IEEE Commun. Mag.*, vol. 51, no. 12, pp. 26–32, Dec. 2013.

[2] L. Grobe *et al.*, "High-speed visible light communication systems,"*IEEE Commun. Mag.*, vol 51, no. 12, pp. 60–66, Dec. 2013.

[3] A. Burton, E. Bentley, H. L. Minh, Z. Ghassemlooy, N. Aslam, and L. Shien-Kuei, "Experimental demonstration of a 10BASE-T Ethernet visible light communications system using white phosphor light-emitting diodes," *IET Circuit, Devices Syst.* vol. 8, no. 4, pp. 322–330, Jul. 2014.

[4] Z. Zhan *et al.*, "1.2 Gbps non-imaging MIMO-OFDM scheme based VLC over indoor lighting LED arrangements," in *Proc. 20th Optoelectron. Commun. Conf.*, Shanghai, China, 2015, pp. 1–3.

[5] N. Fujimoto and H. Mochizuki, "477 Mbit/s visible light transmission based on OOK-NRZ modulation using a single commercially available visible LED and a practical LED driver with a pre-emphasis," presented at *Opt. Fiber Commun. Con. Exp. and the Nat. Fiber Optic Eng. Con.*, 2013, pp. 1–3.

[6] L. Riche, K. Sujaee, and R. George, "The performance of high order modulation QAM-OFDM in the presence mutipath fading channels," in *Proc. IEEE Southeastcon*, 2012, pp. 1–3.

[7] S. Mallick and S. P. Majumder, "Performance analysis of an OFDM system in the presence of Carrier Frequency Offset, phase noise and timing jitter over rayleigh fading channels," in *Proc. Int. Conf. Electric. Comput. Eng.*, 2009, pp. 205–210.

[8] A. M. Khalid *et al.*, "1-Gb/s transmission over a phosphorescent white LED by using rate-adaptive discrete multitone modulation," *IEEE Photonics J.*, vol. 4, no. 5, pp. 1465–1473, Oct. 2012.

[9] G. Cossu *et al.*, "3.4 Gbit/s visible optical wireless transmission based on RGB LED," *Opt. Exp.*, vol. 20, no. 26, pp. 501–506, 2012.

[10] A. H. Azhar, T. Tran, and D. O'Brien, "A gigabit/s indoor wireless transmission using MIMO-OFDM visible-light communications," *IEEE Photonics Technol. Lett.*, vol. 25, no. 2, pp. 171–174, Jan. 2013.

[11] S. Nedic, "An approach to data-driven echo cancellation in OQAM-based multicarrier data transmission," *IEEE Trans. Commun.*, vol. 48, no. 7, pp. 1077–1082, Jul. 2000.

[12] H. Bölcskei, "Orthogonal frequency division multiplexing based on offset QAM," *Advances in Gabor Theory*. Berlin, Germany: Springer, 2003, pp. 321–352.

[13] *Wideband Air Interface Isotropic Orthogonal Transform Algorithm (IOTA)—Public Safety Wideband Data Standards Project—Digital Radio Technical Standards*, TIA-902.BBAB (Physical Layer Specification, Mar. 2003) and TIA-902.BBAD (Radio Channel Coding (CHC) Specification, Aug. 2003), TIA Committee TR-8.5. [Online]. Available: http://www.tiaonline.org/standards/

[14] M. Bellec and P. Pirat, *OQAM Performances and Complexity*, IEEE P802.22, Wireless Regional Area Network, 2006.

[15] L. Zhaohui *et al.*, " Experimental demonstration of 110-Gb/s unsynchronized band-multiplexed superchannel coherent optical OFDM/OQAM system," *Opt. Exp.*, vol. 21, pp. 21924–21931, 2013.

[16] Li, Chao *et al.*, "Experimental demonstration of 429.96-Gb/s OFDM/OQAM–64QAM over 400-km SSMF transmission within a 50-GHz Grid," *IEEE Photonics J.*, vol. 6, no. 4, pp. 1–8, Aug. 2014.

[17] X. Fang *et al.*, "Frequency-domain channel estimation for polarization-division-multiplexed CO-OFDM/OQAM systems," *J. Lightw. Technol.*, vol. 33, no. 13, pp. 2743–2750, Jul. 2015.

[18] B. L. Floch, M. Alard, and C. Berrou, "Coded orthogonal frequency division multiplex [TV broadcasting]," *Proc. IEEE*, vol. 83, no. 6, pp. 982–996, Jun. 1995.

[19] C. Lélé *et al.*, "Channel estimation methods for preamble-based OFDM/OQAM modulations," *Eur. Trans. Telecommun.*, vol. 19, no. 7, pp. 741–750, 2008.

[20] M. K. Ozdemir and H. Arslan, “Channel estimation for wireless OFDM systems,” *IEEE Commun. Surveys Tuts.*, vol. 9, no. 2, pp. 18–48, Apr. 2007.
[21] O. Edfors, M. Sandell, J.-J. van de Beek, S. K. Wilson, and P. O. Börjesson, “OFDM channel estimation by singular value decomposition,” *IEEE Trans. Commun.*, vol. 46, no. 7, pp. 931–939, Jul. 1998.
[22] A. H. Azhar, T. A. Tran, and D. O’Brien, “A gigabit/s indoor wireless transmission using MIMO-OFDM visible-light communications,” *IEEE Photonics Technol Lett*, vol. 25, no. 2, pp. 171–174, Jan. 2013.
[23] J. Vucic, C. Kottke, K. Habel, and K.-D. Langer, “803 Mbit/s visible light WDM link based on DMT modulation of a single RGB LED luminary,” in *Proc. Opt. Fiber Commun. Conf. Expo. Nat. Fiber Optic Eng. Conf.*, 2011, pp. 1–3.